THE ASTROPHYSICAL JOURNAL, 226:947–962, 1978 December 15

THE ENRICHMENT OF HELIUM IN PLANETARY NEBULAE

JAMES B. KALER
University of Illinois Observatory
Received 1978 April 19; accepted 1978 June 22

ABSTRACT

New photoelectric measurements made with interference filters are presented for 36 planetary nebulae in one or more of the following emission lines: Hβ, λ4959 [O III], λ4686 He II, λ4471 He I, and λ3727 [O II]. *B* and/or *V* magnitudes are also given for 31 central stars. Absolute Hβ fluxes for 35 nebulae are tied to the NGC 7027 observation of Capriotti and Daub and to the fluxes presented by Barker.

Several recent papers suggest that a radial galactic gradient exists in He/H. In combination with the data from an earlier paper, this paper provides an independent study of 31 nebulae which also shows a general decrease of He/H away from the galactic center. The combined data (from the Peimberts, Barker, and this paper) show that average He/H is dependent not only upon distance from the galactic center but also upon distance from the galactic plane, and radial velocity.

The data indicate that there is little or no true radial *interstellar* gradient in He/H. The apparent gradient can be explained by a combination of the following two causes. (1) Planetaries are commonly enriched in helium by convective dredging in their parent stars before ejection. The most highly enriched planetaries are found within 12 kpc of the galactic center, which may reflect a greater range of initial stellar masses present. (2) The initial He/H of the halo stars appears to be 15%–20% lower than that of the disk stars. This difference can be reflected into an apparent radial gradient, since most of the nebulae far from the galactic center also have halo characteristics.

Subject headings: galaxies: Milky Way — nebulae: abundances — nebulae: planetary

I. INTRODUCTION

Differences in helium to hydrogen ratios among planetary nebulae are widely recognized, and systematic galactic effects have been discovered. Kaler (1974) found two planetaries with very high He/H (>0.15). D'Odorico, Peimbert, and Sabbadin (1976) and later Torres-Peimbert and Peimbert (1977, hereafter T) found that He/H in planetaries decreases outwardly from the galactic center. They interpreted this as being due to an interstellar He/H abundance gradient. Both Aller (1976) and Barker (1978*a*, hereafter B) found marginal supportive evidence for an observed gradient. Further support for an interstellar gradient comes from Peimbert, Torres-Peimbert, and Rayo (1978), who examined galactic diffuse nebulae, and from Shields and Searle (1978), who studied three diffuse nebulae in M101. However, the concept of an interstellar gradient is in conflict with the helium line intensities observed by Smith (1975) in other spiral galaxies (to which no model for the determination of neutral helium was applied) and with the observations of galactic nebulae by Hawley (1978), who found no such gradient. The measurement of the interstellar gradient is a difficult problem. In the case of diffuse nebulae we must apply models in order to estimate the amount of unseen neutral helium present, and in the case of planetaries the helium observed may have been enhanced by fusion processes in the parent star.

It is the purpose of this paper to examine the origin of the variation of He/H among planetaries. In the process, the λ4471 line of He I has been observed for 24 nebulae. These observations, combined with those of Kaler (1976*a*, hereafter Paper I) and with λ4686 He II observations by others, provide an independent study of 31 planetaries. Also, as part of the observing program, F(Hβ), $I(\lambda4959)$[O III]/I(Hβ) and central star magnitudes are found for most of the nebulae.

There are now three large comparable studies of He/H in planetary nebulae, this paper (31 nebulae), T combined with earlier measurements by Peimbert and Torres-Peimbert (1971, hereafter P) (43 nebulae), and B (35 nebulae). The combined data yield information on 78 objects. These data, together with data from selected other studies, are then used for a detailed examination of He/H ratios. The observations are presented in § II, and the new (this paper) helium to hydrogen ratios are discussed in § III. The combined data and the results derived therefrom are given in § IV. Finally, § V presents a summary and the conclusions.

II. THE OBSERVATIONS

This paper continues the earlier work published in Paper I. The procedures for observation and reduction are identical to those used there, and the reader should refer to it for details. All observations were made at the University of Illinois Prairie Observatory.

The observations are presented in Table 1. The first three columns present, in order, the nebula's common name, the Perek-Kohoutek (1967) number, and the log

TABLE 1

Observed Fluxes and Central Star Magnitudes

Nebula (1)	PK (2)	- log F(Hβ) ergs cm^{-2} sec^{-1} (3)	Relative Line Fluxes I(Hβ) = 100 λ4959 [OIII] (4)	λ4471 He I (5)	λ3727 [OII] (6)	B (7)	V (8)	Nights (9)	Notes (10)
NGC 246	118 - 74°1	10.53 ± .05*						1	
650-1	130 - 10°1	10.68 ± .01†		3.6 ± .3		15.9 ± .5	16.3 ± .5	3	
1360	220 - 53°1	10.2 ± .1*†				11.00 ± .03	11.34 ± .01	1	1
2371-2	189 + 19°1	11.00 ± .02†		1.3 ± .5		14.7 ± .1	14.8 ± .1	1	
2440	234 + 2°1	10.50 ± .01‡		3.2 ± .3		15.2 ± .4	14.0 ± .2	3	2
2474-5	164 + 31°1					16.5 ± .2	16.0 ± .2	1	
3242	261 + 32°1			3.7 ± .1				3	
6058	64 + 48°1	11.77 ± .01	355 ± 18	0.9 ± 1.0		13.6 ± .1	13.4 ± .1	2	3
6210	43 + 37°1	10.08 ± .01	355 ± 5	4.8 ± .1		12.0 ± .1	12.3 ± .1	2	
6309	9 + 14°1	11.19 ± .08	355 ± 70				14.4 ± .1	1	
6543	96 + 29°1	9.61 ± .01		6.2 ± .1		10.93 ± .05	10.93 ± .07	2	
6741	33 - 2°1	11.32 ± .01		4.2 ± .5		16.0 ± .7	14.7 ± .4	2	4
6803	46 - 4°1	11.19 ± .01	358 ± 64			$16^{-\infty}_{+1}$	15.2 ± .2	1	
6826	83 + 12°1	9.98 ± .01		5.1 ± .1		10.2 ± .1	10.6 ± .1	1	
6884	82 + 7°1	11.11 ± .01				15.8 ± .2	15.7 ± .1	1	
6886	60 - 7°2	11.32 ± .02		4 ± 2			15.7 ± 1.0	1	
NGC 7354	107 + 2°1	11.57 ± .01		2.3 ± .4		16.1 ± .5	15.0 ± .2	1	
IC 1454	117 + 18°1	12.17 ± .03*	470 ± 50		79 ± 17	18 ± 2	16.4 ± .5	2	5
1747	130 + 1°1	11.49 ± .01		2.8 ± .4		15.8 ± .6	15.4 ± .1	1	
2003	161 - 14°1	11.20 ± .01		2.7 ± .1		15.3 ± .3	15.4 ± .1	2	
2120	169 - 0°1	12.2 ± .1*	40 ± 40					2	
4593	25 + 40°1	10.59 ± .01		5.3 ± .9		10.98 ± .05	11.24 ± .05	1	
4732	10 - 6°1	11.50 ± .02	605 ± 33	4.7 ± .7		16.9 ± .8	16.7 ± .5	3	
4997	58 - 10°1	10.54 ± .01	197 ± 13	5.1 ± .4		14.6 ± .6	14.3 ± .2	1	
5117	89 - 5°1	11.37 ± .01		3.9 ± .3		17.2 ± .5	15.7 ± .5	2	6
IC 5217	100 - 5°1	11.19 ± .01		$4.5^{+1.6}_{-2.0}$		15.4 ± .1	15.5 ± .1	2	
A 2	122 - 4°1	12.34 ± .03*	445 ± 45				16 ± 1	1	
A 35	303 + 40°1	11.1: ± .2*†	115 ± 20		600 ± 100			1	7
A 78	81 - 14°1	12.2 ± .1*	400 ± 300			12.3 ± .1	12.8 ± .1	1	
Ba 1	171 - 25°1	12.44 ± .02*					> 17	1	
Hu 2-1	51 + 9°1	10.78 ± .01		3.6 ± .2		13.4 ± .1	13.34 ± .02	1	
J 320	190 - 17°1	11.37 ± .01		5.0 ± .3		14.2 ± .1	14.4 ± .1	3	
J 900	194 + 2°1	11.21 ± .01	360 ± 10	2.45 ± .15		16.2 ± .2	15.3 ± .1	2	8
M 1-79	93 - 2°1	11.88 ± .02*	245 ± 22					1	
Me 2-1	342 + 27°1	11.36 ± .03‡		0.9 ± .9		17.3 ± .8‡	16.7 ± .3‡	2	9
Sn - 1	13 + 32°1	11.73 ± .02	350 ± 20	4.1 ± .7	30 ± 5	14.4 ± .1	14.7 ± .1	2	
Vy 1-1‡	118 - 8°1	11.54 ± .01	296 ± 20	5.5 ± .5		14.1 ± .2	14.3 ± .1	2	

Notes to Table 1

* First photoelectrically measured Hβ flux.

† Correction for photometer beam applied (see Paper I).

‡ Replaces measurements given by Paper I.

[1] NGC 1360 larger than 4′ aperture used; object observed at several positions, and beam shape correction applied.
[2] NGC 2440 larger than 40″ aperture used. Flux is somewhat (probably < 10%) greater than given here.
[3] 10% correction applied to log $F(H\beta)$ because of the stellar absorption line.
[4] 48% brighter than given by Collins, Daub, and O'Dell (1961).
[5] $I(\lambda 4686)$ He II = 24 ± 4.
[6] 2.19 times brighter than given by O'Dell (1963); the present value agrees with that measured by Vorontsov-Vel'yaminov *et al.* (1965).
[7] A35 larger than 4′ aperture. Object observed at one position and flux estimated from surface brightness, so the value is quite approximate.
[8] Nearby star may affect *B* and *V*.
[9] Magnitudes given by Paper I apparently included a nearby field star.

of the Hβ flux (uncorrected for He II Pickering 8 contamination). All values in column (3) are total Hβ fluxes except that of NGC 2440, for which the 40″ aperture cut off part of the faint outer halo. NGC 1360 and A35 were both larger than the largest aperture available (4′), and the fluxes had to be estimated from surface-brightness measurements. NGC 1360 was measured at nine positions; thus the entire nebula was observed, but only the brightest part of A35 was observed, so that its flux is only an estimate. No allowance was made for possible central star absorption lines, except for NGC 6058 for which an Hβ equivalent width of 5 Å was estimated from Aller (1968).

The fluxes in Paper I were tied to Miller and Mathews's (1972) measurement of $F(\mathrm{H}\beta)$ for NGC 7027, which is 0.07 in the log fainter than that measured by Capriotti and Duab (1960). Consequently all of the new fluxes were lower, by the same amount, than the older values, represented, for example, by O'Dell (1962, 1963). However, absolute calibration changes can account for at most only half of this difference. The Hβ fluxes for eight of the nebulae from this work and Paper I were also observed by B, who used the same stellar photometric system (Oke and Schild 1970) as Miller and Mathews (1972). Yet agreement between the new fluxes and B's fluxes (to about 0.01 in the log) is obtained if Capriotti and Daub's (1960) calibration is used; if Miller and Mathews's (1972) NGC 7027 flux is used, the new fluxes are 0.08 (in the log) fainter than B's. In addition, direct comparison between six of B's fluxes and those of O'Dell (1962, 1963) shows agreement to 0.01 in the log. Because of the consistency between B's results and the older fluxes, it appears that Miller and Mathews (1972) underestimated log $F(\mathrm{H}\beta)$ for NGC 7027 by ~ 0.07. Consequently, the fluxes in Table 1 are tied to Capriotti and Daub's (1960) measurement for this object. All values of log $F(\mathrm{H}\beta)$ in Paper I should be increased by 0.07. Two nebulae (NGC 6741 and IC 5117) are found to have significantly different fluxes from those measured previously (see the notes to Table 1).

The next three columns of Table 1 give the relative fluxes for the λ4959 [O III], λ4471 He I, and λ3727 [O II] lines, on the scale $F(\mathrm{H}\beta) = 100$. These values are not corrected for interstellar reddening. For IC 1454 λ4686 He II was observed; its relative flux is given in note 5 to Table 1.

Columns (7) and (8) give a measure of B and V for the central star of the nebula. B is determined from a continuum filter at λ4428, and V from the Strömgren y filter, which is nearly free of emission lines.

The last two columns of Table 1 give the number of nights on which each nebula was observed, and references to various notes placed at the end of the table. In some instances the measurements of Table 1 replace those given in Paper I.

The errors are the formal mean errors of the mean calculated from the counting statistics of a given night, or derived from the comparison of multiple-night observations. Systematic errors are of particular importance for B and V, especially for stars fainter than 15th mag, but they cannot as yet be evaluated. The reader is simply cautioned that they may well be present.

III. HELIUM TO HYDROGEN RATIOS

a) General Calculations

Helium to hydrogen ratios are calculated in a straightforward manner from the effective radiative recombination coefficients given by Brocklehurst (1971, 1972). He^{2+}/H^+ is found from λ4686 He II, and He^+/H^+ is calculated here from λ4471, λ5876, and λ6678 of He I. There has been considerable discussion for the past several years about the influence of collisional excitation and self-absorption on the He^+ triplet lines λ5876 and λ4471 (Cox and Daltabuit 1971). Both T and B show that collisional excitation can be disregarded, but that the triplets must be corrected for self-absorption. The degree of the correction is related to $\tau(\lambda 3889)$, which can be found by comparing the observed and calculated values of $I(\lambda 7065)/I(\lambda 4471)$ and $I(\lambda 7065)/I(\lambda 5876)$. T used the calculations of Robbins (1968), normalized to the maximum self-absorption calculated by Cox and Daltabuit (1971).

Unfortunately, λ7065 is available for only about half of the total number of nebulae considered in this paper, so that some other measure of $\tau(\lambda 3889)$ must be found. It seems reasonable that this quantity should in some way be proportional to the density of the nebula. Consequently, $\tau(3889)$ was calculated for all the nebulae for which λ7065 is observed and for which the density is known from the nebular [O II] and/or [Cl III] ratios. Data were taken from Kaler's (1976*b*) catalog (hereafter KC), T, B, and Hawley and Miller (1978); the necessary extinctions and electron temperatures were calculated from these data as well.

The results are presented in Figure 1, in which $\tau(3889)$ is plotted against log N_e (which is the mean of

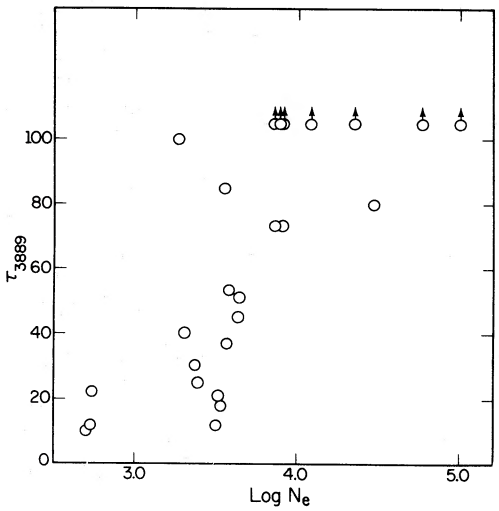

FIG. 1.—Optical depth, τ, at He I λ3889 as a function of electron density.

the [O II], [Cl III] values). The scatter is fairly large, but a clear relation is discernible. The nebulae with $N_e > 10^4$ cm^{-3} exhibit essentially maximum self-absorption, whereas those with $N_e < 10^3$ cm^{+3} show only a small amount. In this paper, corrections are first made to the λ4471 and λ5876 line intensities (for $3 \leq \log N_e \leq 4$) according to

$$I_{\rm rad}(\lambda) = I_{\rm obs}(\lambda)/[1 + \gamma_{\rm SA}({\rm max})(\log N_e - 3)] \quad (1)$$

where $I_{\rm obs}$ is the observed relative intensity, $I_{\rm rad}$ is the intensity for pure radiative equilibrium with no self-absorption, and $\gamma_{\rm SA}$(max) is the maximum self-absorption from Cox and Daltabuit (1971). This correction is made for all nebulae treated in this paper. Since the correction is always small to start with (typically ~6% for λ5876, ~3% for λ4471), equation (1) should be adequate to well within the observational errors.

The final He/H ratios are calculated according to the [O III] electron temperature of the nebula, as opposed to the [N II] temperature. Kaler (1978*a*) showed that [Ar III] temperatures are more closely correlated with the [O III] temperatures. Since He^+ and Ar^{2+} have similar lower ionization potentials, T_e [O III] is probably more appropriate to He^+/H^+. Finally, all observations are corrected for the He II Pickering 8 blend with Hβ, as calculated from I(λ4686) and Brocklehurst (1971).

b) Helium to Hydrogen from the Prairie Data

Helium to hydrogen ratios calculated for the nebulae of Table 1 and Paper I according to the scheme in § III*a* are presented in Table 2. Densities, temperatures, and extinction constants are discussed in the next section and are given in Table 3. Column (1) gives the nebula's name, and column (2) gives He^+/H^+ calculated from the data in Table 1 and Paper I. For the values of He^{2+}/H^+ given in column (3), under half of the data come from the present filter photometry. For the other objects (marked with an asterisk in col. [3]), I(λ4686) was taken from the literature previously cited. The error is derived from the scatter in these observations. This procedure is acceptable because the λ4686 line is strong, easily observed, and generally accurately known. The accuracy of total He/H ratios is controlled

TABLE 2

He/H FROM THIS PAPER AND PAPER I

Nebula (1)	He^+/H^+ (2)	He^{2+}/H^+ (3)	He/H (4)	Remarks (5)
NGC 650	.077 ± .006	.054 ± .002*	.131 ± .007	
2371	.028 ± .010	.093 ± .009*	.121 ± .014	
2440	.073 ± .007	.065 ± .004*	.138 ± .008	
3242	.077 ± .002	.032 ± .001	.109 ± .003	
3587	.074 ± .004	.009 ± .001	.083 ± .004	
4361	.024 ± .009	.111 ± .005	.135 ± .011	
6210	.097 ± .004	.002*	.099 ± .004	THICK
6543	.123 ± .002	—	.123 ± .002	
6741	.095 ± .013	.041 ± .004*	.136 ± .014	
6826	.104 ± .002	—	.104 ± .002	
6833	.101 ± .013	.002*	.103 ± .013	THICK
6886	.088 ± .045	.037 ± .002*	.125 ± .045	
7026	.093 ± .010	.009 ± .014	.102 ± .014	
NGC 7354	.075 ± .024	.057 ± .013*	.132 ± .028	
IC 1747	.067 ± .010	.019 ± .002*	.086 ± .010	
2003	.063 ± .003	.048 ± .002*	.111 ± .004	
2165	.060 ± .005	.036 ± .003	.096 ± .006	
3568	.092 ± .010	.001*	.093 ± .010	
4593	.105 ± .018	—	.105 ± .018	THICK, He^o
4732	.117 ± .019	—	.117 ± .019	THICK
4997	.117 ± .009	—	.117 ± .009	THICK
5117	.107 ± .012	.012 ± .002*	.119 ± .012	THICK
IC 5217	$.093^{+.03}_{-.04}$	.007*	$.100^{+.030}_{-.040}$	
Hu 1 - 1	.064 ± .013	.008 ± .001	.072 ± .013	
Hu 1 - 2	.073 ± .012	.097 ± .005	.170 ± .013	
Hu 2 - 1	.078 ± .005	—	.078 ± .005	THICK, He^o
J 320	.108 ± .007	.001*	.109 ± .007	
J 900	.055 ± .005	.041 ± .005*	.096 ± .007	
Me 2 - 2	.167 ± .012	—	.167 ± .019	THICK
Sn - 1	.086 ± .015	.002*	.088 ± .015	
Vy 1 - 1	.139 ± .020	—	.139 ± .020	THICK

*He^{2+}/H^+ derived from observations in KC, plus T and B.

by the accuracy of measurement of the much weaker He I lines. The only problem is that of stratification, since the He I line is usually appropriate to the whole nebula, whereas the He II observations often come from slit spectrograms. An attempt was made to choose and average the observations such that $I(\lambda 4686)$ is appropriate to the whole object.

Column (4) of Table 2 contains the total He/H, where the errors are added quadratically. The remarks, column (5), indicate whether the nebula is expected to be optically thick, and whether neutral helium is expected to be present (indicated by He^0). Neutral helium should not be a problem except for IC 4593 and Hu 2–1, and possibly NGC 3587 (see below). Criteria for optical depth and the neutral helium problem are discussed in § IV*b*.

About half of the objects of Table 2 have been accurately observed by others. The accuracy of the filter photometry from Prairie Observatory is evaluated in Figure 2, by plotting the He/H of Table 2 [called He/H (K) to denote this paper and Paper I] against He/H derived from T, B, and Lutz (1977). The errors in He/H (other) are derived from the scatter in He^+/H^+ found from the three He I lines considered. Except for three nebulae, the agreement is excellent. These three, in order of increasing He/H, are Hu 1–1, NGC 3587, and IC 2165. The source of disagreement for Hu 1–1 and IC 2165 is not understood. The Prairie intensities for $\lambda 4471$ and $\lambda 4686$ of Hu 1–1 are both less than those observed by B. In the case of IC 2165, the difference is all in the $\lambda 4471$ line. This line was observed at Prairie on three nights over a 5 year period with good internal agreement. On the other hand, T observed three He I lines, also with good internal agreement. NGC 3587 is a different matter. The Prairie intensities for both He I and He II are less than those observed by T; He I was observed at Prairie on three nights, He II on five nights, with very good internal agreement. T observed both He I and He II at the center of the nebula, but the Prairie observations encompassed the whole object; the latter also show He II increasing toward the center (see Paper I). The comparison between Paper I and T is what would be expected if NGC 3587 were optically thick and if the He^+ Strömgren sphere were less than the H^+ sphere, that is, if NGC 3587 contained neutral helium. The nebula is unusual in this set of observations because of the very low luminosity of the central star. This hypothesis is not certain, and it should be tested further by examining the distribution of the He I line flux. The dashed line in Figure 1 is a least-squares fit through all the points except NGC 3587. The agreement shows that there is no significant systematic error in the filter calibrations.

The data of Table 2 now provide a fairly independent test of a galactic helium gradient. The He/H ratios are plotted against distance from the galactic center projected onto the plane R in Figure 3. The sizes of the points inversely reflect the size of the error, according to the legend in Figure 3. Optically thick points are indicated by crosses, and IC 4593 and Hu 2–1 (which may contain He^0) are excluded.

Values of R for optically thin nebulae are derived from Cahn and Kaler (1971), modified for the new fluxes and observed extinction coefficients (derived from KC, T, and B). The distances of the thick nebulae are derived from the scheme outlined by Cudworth (1974), divided by 1.45 to put them on the Cahn and Kaler scale. The validity of either of these distance scales is still an open question. For the purposes of this paper, it is only important that one self-consistent scheme be chosen. The Sun is placed at 10 kpc from the galactic center. Values of R are given in Table 3.

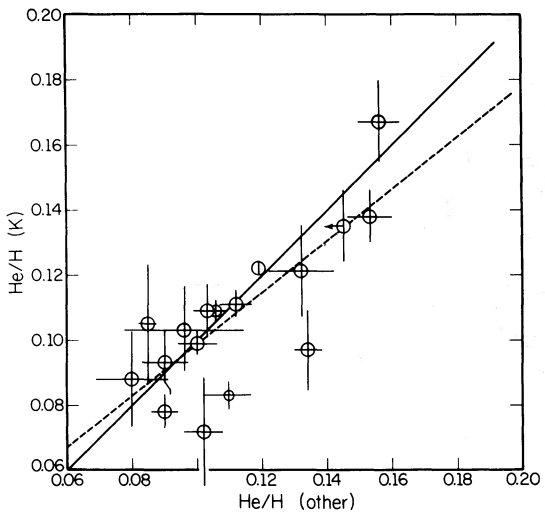

FIG. 2.—He/H from the data of this paper, Table 2, plotted against other accurately determined values.

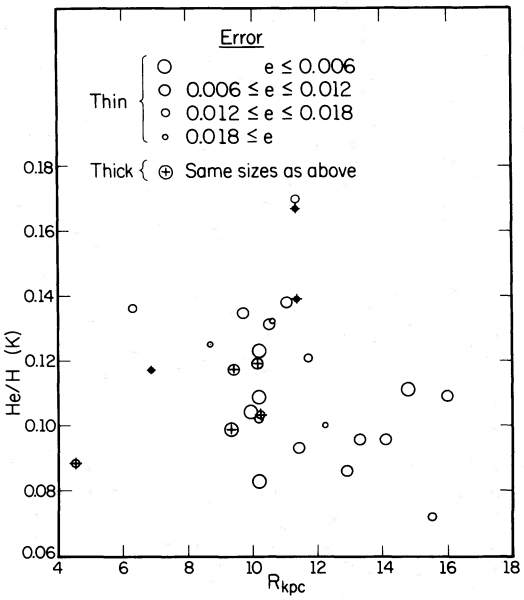

FIG. 3.—He/H from Table 2 (this paper) plotted against distance from the galactic center as projected onto the galactic plane. The crosses are optically thick nebulae. The size of the symbol is inversely related to the error (see the legend in the inset).

An apparent gradient, consistent with that found by T, is seen in Figure 3. An unweighted least-squares fit through all the points (except those for which the error $\geq \pm 0.02$) indicates a gradient of about -0.0016 kpc^{-1}, less than one-third that found by T. It is somewhat steeper (-0.0020 kpc^{-1}) if only the optically thin points are chosen.

The problem with establishing a true gradient from these data is that some planetaries are known to have had their helium content enhanced by nuclear burning processes; witness the high values of Hu 1–2, Me 2–2 and even NGC 2440. In order to determine whether a true gradient exists, we must eliminate the helium-enhanced objects. But we do not know which ones they are. If a planetary can have its helium enhanced by a large amount, as in Hu 1–2, it certainly can have it enhanced by a small amount. An alternate way of viewing Figure 3 is to note that at the Sun the spread in He/H is large, from low to high values, but that beyond ~ 12 kpc, most of the nebulae have normal, unenhanced He/H. For $R < 12$ kpc, there are an equal number of nebulae with He/H greater than and less than 0.12. But for $R < 12$ kpc, all seven objects have He/H < 0.12. The data suggest that nebulae in the solar neighborhood are more likely to be enriched in helium than are the nebulae farther from the galactic center, although an interstellar gradient may exist as well.

As an illustration of the hazards of using a small number of points, note that a gradient determined from the optically *thick* nebulae goes in the opposite direction. It is obviously of importance to increase the number of points, with as little preselection (on the basis of He/H) as possible. In the next section, the three data sets already discussed are combined for a more detailed study than any single observer has been able to carry out.

IV. THE COMBINED DATA

a) Helium to Hydrogen Ratios

The principal data are assembled from this paper, Paper I, T, P, and B. Also selected are the observations of Lutz (1977), used to improve the precision for three objects, and data for six other objects: the low-excitation object NGC 40 from Aller *et al.* (1972), and the two high He/H nebulae NGC 6445 and NGC 6302 from Aller *et al.* (1973), Danziger, Frogel, and Persson (1973), and Oliver and Aller (1969), and the three extreme halo planetaries from Hawley and Miller (1978).

Data and results are presented in Table 3. The first four columns give the nebula's name, interstellar extinction constant, c, the [O III] electron temperature times 10^{-4}, t, and the log of the electron density, N_e. These quantities are derived from the literature cited earlier. If an [O III] temperature is not available, the [N II] temperature is adopted. Values of N_e are preferably derived from nebular [O II] or [Cl III] ratios, but if these are not available, other forbidden-line data are used, or an rms value based upon the distance is assumed.

Values of He^+/H^+, He^{2+}/H^+, He/H and the references used are given in columns (5) through (8), respectively. The He/H ratios are calculated according to the scheme of the last section, and He^+/H^+ values are calculated from λ4471, λ5876, and λ6678 when available. The key to the references is given at the end of Table 3. About 30% of the objects are observed more than once, in which case the individual He/H are generally, but not always, averaged as follows: if all three He I lines are observed by T and B, then K and B are given equal weight, and T given double weight. Otherwise, K and T are given equal weight and B given half-weight. Double weight is indicated by an asterisk in column (8). The results for NGC 3587 are a straight average of the K and T data (see § III*b*). This weighting system was determined by comparing different observers' data (external comparison) and by intercomparing one observer's results based upon the different He I lines (internal comparison). The errors in columns (5), (6), and (7) are also determined from internal or (preferably) external comparisons. In the case of the Prairie Observations (K), they are taken from Table 1 and Paper I. In some cases errors are placed on total He/H but were not placed on He^+ or He^{2+} because of stratification or lack of data, or because He^{2+} was too small to warrant it. When no comparisons were available the error in He/H was estimated from the authors' comments.

b) Neutral Helium and Optical Depth

Before we can examine trends in He/H, we must first eliminate those nebulae which contain significant amounts of neutral helium. The neutral state will most obviously exist for nebulae with low central star temperatures, although it cannot be ruled out for higher-excitation objects. We might also expect it to be present for optically thick nebulae in general. Columns (9) and (10) of Table 3 give Ex = He^{2+}/He or log T_* (from Kaler 1976*c*, 1978*b*), and an indication of whether the nebula is expected to be optically thick, indicated by a "T." An "S" in column (10) indicates that the nebula is stellar, and has no measured angular extent. A nebula was called *thick* if it met the following criteria:

1. $He^{2+}/H^+ < 0.005$, that is, no more than a trace of He^{2+} is present. See, for example, Hummer and Seaton (1964). Exceptions are nebulae with observed outer halos, e.g., NGC 6543, planetaries with $0 < He^{2+}/H^+ < 0.005$ but which have radii > 0.09 pc (modified from Cahn and Kaler 1971), and Ps 1, which has a very low mass (see Peimbert 1973). These objects are considered to be thin.

2. The nebulae are stellar; all but IC 5217 also meet the criteria above.

These criteria are certainly not absolute, but they seem at least generally reasonable; they are conservatively adopted so as to increase the certainty of selection of thin nebulae, which are more likely to have no neutral helium.

Helium to hydrogen ratios are plotted against log T_* on the left side of Figure 4, for all nebulae with measured T_*. Log T_* for Ps 1 is almost certainly a

TABLE 3

COMPILATION OF He/H VALUES

Nebula (1)	c (2)	t (3)	log Ne (4)	He^+/H^+ (5)	He^{2+}/H^+ (6)	He/H (7)	Refs (8)	Log T_* / Ex (9)	τ (10)	R kpc (11)	|Z| kpc (12)	$\|v_r\|$ km/sec (13)	Morph (14)	Pop. (15)	Rmks (16)
NGC 40	.28	1.17	3.33	.070 ± .015:	—	.070 ± .015:	A	4.50						I	
650	.15	1.18	3.75	.077 ± .006	.054 ± .002	.131 ± .007	K	.41		10.5	.14	23	B	I'	
1535	.13	1.17	3.50	.085 ± .005	.011	.096 ± .002	P,T	.11		11.4	1.35	6	N	II	
2022	.65	1.55	3.24	.016	.105	.121 ± .017	T	.87		12.4	.49	14	N	II	
2371	.07	1.45	3.71	.028 ± .007	.098 ± .005	.126 ± .005	K,T	.78		11.7	.61	20	B	I	
2392	.16	1.42	3.43	.049 ± .004	.043 ± .002	.092 ± .005	B,T	.53		11.1	.36	81	N	II	
2438	.20	1.04	3.30	.067	.036	.103 ± .01	T	.35		10.9	.10	77	N	II	
2440	.17	1.30	3.11	.089 ± .015	.057 ± .007	.146 ± .003	K,T*	.39		11.0	.07	63	B	I'	1
2452	.55	1.30	3.07	.041	.071	.112 ± .01	T	.63		11.7	.05	68	B	I'	
2610	.12	1.68	< 3	.029 ± .003	.081	.110 ± .005	T	.74		11.4	.60	88	N	II	
2792	.69	1.38	3.04	.033	.083	.116 ± .01	T	.72		10.8	.24	14	(N)	I'	
3132	.25	0.99	< 3	.122 ± .003	.004	.126 ± .003	T	.03		10.0	.26	7	N	I'	1
3211	.34	1.37	< 3	.076	.076	.152 ± .015	T	.50		9.6	.26	20	(N)	I'	
3242	.05	1.13	3.54	.078 ± .005	.029 ± .005	.107 ± .002	B,K,T*	.27		10.2	.63	5	N	I	
3587	.01	1.11	< 3	.083 ± .009	.014 ± .015	.097 ± .010	K, T	.17		10.2	.44	7	N	I	2
3918	.36	1.18	> 4	.070 ± .004	.038	.108 ± .006	T	.35		9.4	.13	16	B	I'	
4361	.04	1.97	< 3	.024 ± .009	.111 ± .005	.135 ± .011	K	.82		9.7	.70	10	N	I	
5307	.59	1.30	3.36	.072 ± .003	.025	.097 ± .004	T	.26		8.3	.55	40	N	I	
5315	.55	0.84	> 4	.123 ± .003	.004	.127 ± .003	T	4.75	T	9.4	.08	23	N	I'	
5882	.38	0.93	3.58	.113 ± .003	.003	.116 ± .003	T	4.79	T	9.0	.21	8	N	I'	
6210	.09	0.96	3.71	.097 ± .003	.002	.099 ± .003	B,K*	4.76	T	9.3	.74	37	N	I	
6302	1.33	2.00	> 4	.161	.064	.225	D, A	.28		9.1	.02	37	B	I'	
6445	.50	1.30	3.36	.165 ± .020:	.061 ± .005	.226 ± .02:	A	.27		8.1	.13	16	B	I'	
6543	.18	0.81	3.86	.121 ± .002	—	.121 ± .002	K,L	4.65		10.2	.78	65	N	I	
6567	.40	1.06	3.46	.120 ± .005	.002	.122 ± .005	B	4.75	T	7.8	.03	120	N	II	
6572	.41	1.05	> 4	.110 ± .005	—	.110 ± .005	P	4.78	T	9.5	.12	10	N	I'	
6644	.41	1.22	3.87	.102 ± .003	.015	.117 ± .004	B	.13	T	7.7	.29	194	N	II	3
6720	.12	1.15	< 3	.075 ± .007	.038	.113 ± .008	P	.28		9.7	.20	21	B	I'	
6741	.45	1.11	3.80	.095 ± .013	.041 ± .004	.136 ± .014	K	.30		6.5	.23	41	B	I'	
6803	.60	1.02	3.89	.124 ± .003	.003	.127 ± .003	P	4.79	T	8.4	.17	13	N	I'	
6826	.04	0.97	3.21	.104 ± .002	—	.104 ± .002	K	4.67		9.9	.33	6	N	I'	
6833	.24	1.27	3.99	.095 ± .004	.002	.097 ± .004	B,K	4.69	S	10.2	.77	108	N	II	
6884	.81	0.92	3.90	.095	.013	.108 ± .010	P	.12		10.3	.48	36	N	I	
6886	.66	1.29	> 4	.088 ± .045	0.37 ± .002	.125 ± .045	K	.30		8.7	.55	35	B	I	
NGC 7009	.17	1.04	3.64	.101 ± .006	.011	.112 ± .006	P	.10		9.2	.72	47	N	I	
7026	.86	1.03	3.86	.092 ± .010	.009 ± .001	.101 ± .010	K	.09		10.2	.02	40	B	I'	
7027	1.37	1.17	> 4	.069 ± .005	.042 ± .003	.111 ± .002	B,P	.38		10.0	.08	11	(N)	I'	
7354	1.8 ± 1	1.35:	3.75:	.075 ± .024	.057 ± .013	.132 ± .028	K	.43		10.6	.07	42	N	I'	
NGC 7662	.19	1.29	3.55	.055	.039	.094 ± .01	P	.42		10.7	.57	11	N	I	
IC 351	.34	1.12	3.72	.064 ± .004	.031 ± .003	.095 ± .002	B,P*	.33		15.3	1.49	10	N	II	

TABLE 3—*Continued*

Nebula (1)	c (2)	t (3)	log Ne (4)	He^+/H^+ (5)	He^{2+}/H^+ (6)	He/H (7)	Refs (8)	Log T_* / Ex (9)	τ (10)	R kpc (11)	|Z| kpc (12)	$\|v_r\|$ km/sec (13)	Morph (14)	Pop. (15)	Rmks (16)
418	.32	0.94	> 4	.076 ± .005	—	.076 ± .005	B,P,T	4.50						I	
1747	.59	1.18	3.57	.067 ± .010	.019 ± .002	.086 ± .010	K	.22		12.9	.10	71	B	II	
2003	.41	1.19	3.57	.061 ± .008	.048 ± .002	.109 ± .007	B,K,T*	.44		14.8	1.33	23	N	II	
2149	.28	1.10	3.26	.076 ± .009	—	.076 ± .009	B,T*	4.56						II	4
2165	.48	1.34	3.64	.078 ± .017	.037 ± .001	.115 ± .016	K,T	.32		13.3	.86	53	B	II	5
2448	.08	1.24	3.25	.073 ± .006	.022	.095 ± .007	T	.23		9.7	1.05	24	N	II	
2501	.55	0.92	> 4	.107 ± .002	.001	.108 ± .002	T	4.71	T	9.8	.13	33	B	I'	
3568	.18	1.08	3.74	.091 ± .005	.001	.092 ± .005	B,K*	4.79		11.4	1.55	41	N	II	
4406	.28	1.05	3.17	.134 ± .002	.007	.141 ± .002	T	.05		8.5	.58	29	B	I	
4593	.08	0.88	3.77	.091 ± .007	—	.091 ± .007	B,K,L	4.64						II	
4732	.64 ± .3	1.58 ± .2	3.43	.117 ± .019	—	.117 ± .019	K	4.81	T	6.8	.37	145	N	II	
4846	.40	0.97	> 4	.086 ± .010	.001	.087 ± .010	B	4.79	S	7.0	.59	151	(N)	II	
4997	.52	2.7	> 4	.117 ± .009	—	.117 ± .009	K	4.69	T	9.4	.24	64	N	I'	
5117	1.33	1.12	> 4	.107 ± .012	.012 ± .002	.119 ± .012	K	.10	S	10.1	.11	26	N	I'	
IC 5217	.35	1.12	3.90	.089 ± .016	.005	.094 ± .010	B,P	.05		12.2	.51	99	N	II	6
BB - 1	.23	1.24	3.28	.079 ± .007	.020	.099 ± .008	H	.20		12.4	19.	196	(N)	II	7
BD +30	.65	0.82	> 4	.044 ± .014	—	.044 ± .014	T	4.43						I	
Cn 3 - 1	.18	0.67	3.51	.041 ± .005	—	.041 ± .005	L,B	4.40						I	
Ha 4 - 1	.14	1.20	< 3	.106 ± .002	.009	.115 ± .003	H	.08		9.7	12.2	141		II	
He 2 -108	.59	1.05	3.06	.102 ± .014	—	.102 ± .014	T	4.47							
He 2 -131	.17	0.64	> 4	.035 ± .003	—	.035 ± .003	T	4.42							
He 2 -138	.23	1.10:	3.59	< .011:	—	< .011:	T	4.34							
Hu 1 - 1	.32	1.07	3.78	.078 ± .008	.012	.090 ± .010	B*,K	.13		15.5	.93	60	B	II	8
Hu 1 - 2	.59	1.94	3.89	.073 ± .012	.097 ± .005	.170 ± .013	K	.57		11.2	.89	10	B	I	
Hu 2 - 1	.51	0.91	3.98	.084 ± .006	—	.084 ± .006	B,K	4.56						I	
J 320	.22	1.25	3.62	.105 ± .006	.001	.106 ± .006	B,K*	4.76		16.0	1.95	234	N	II	
J 900	.35	1.20	3.66	.055 ± .005	.041 ± .005	.096 ± .007	K	.43		14.1	.19	47	B	II	
M 1 - 1	.29	1.41	3.40	.020 ± .002	.092	.112 ± .008	B	.82		16.5	1.7	45	(N)	II	
M 1 - 5	1.48	0.88	3.90	.087 ± .004	—	.087 ± .004	B	4.58						II	9
M 1 - 14	.82	1.02	3.70	.086 ± .003	—	.086 ± .003	T	4.55						II	
M 1 - 74	.81	0.96	3.83	.110 ± .004	—	.110 ± .004	B	4.79	S	8.3	.25	10	(N)	I	
M 2 - 9	1.23	1.34	> 4	.078 ± .008	—	.078 ± .008	B	4.47							
M 2 - 50	.57	1.16	> 4	.073 ± .10	.006	.079 ± .10	B	4.79	T	15.8	.47	136	(N)	II	10
M 3 - 35	2.56	1.06	> 4	.103 ± .007	—	.103 ± .007	B	4.79	T	9.7	.04	163	(N)	II	
Me 2 - 2	.21	1.02	3.91	.162 ± .004	—	.162 ± .004	B*,K	4.66	S	11.3	.58	152		II	
Pb - 4	.56	1.05	3.04	.121	.018	.139 ± .014	T	.13		10.5	.30		N		
Pb - 6	.60	1.40	< 3	.080	.107	.187 ± .018	T	.57		10.4	.42		(B)		
Ps - 1	.26	1.24	3.30	.090 ± .010	—	.090 ± .010	H	4.43		10.1	4.5	139	(N)	II	11
Sn - 1	.22	0.98	3.49	.082 ± .004	.002	.084 ± .004	B,K	4.77	S	4.5	3.8	87	(N)	II	
Vy 1-1	.96 ± .4	1.12	3.5:	.139 ± .020	—	.139 ± .020	K	4.72	S	11.3	.36	14	N	I	

REMARKS TO TABLE 3

[1] Nebulae highly stratified; He^{2+}/He^{+} depends strongly upon position and observer.
[2] NGC 3587 may contain neutral He, as He/H from slit near the center is significantly larger than He/H derived from the whole nebula.
[3] Considered thick because of anomalously high Cahn-Kaler distance.
[4] Large discrepancy in He/H between B(0.098) and T(0.067)
[5] Large discrepancy in He/H between K(0.095) and T(0.130). K observed three nights over 5 years with close agreement; T observed 3 lines with close agreement. Value presented is a straight mean.
[6] Large discrepancy in He/H between B(0.104) and P(0.072); K not used because of large error.
[7] BB 1 = 108−76°1 discovered by Boeshaar and Bond (1977).
[8] K and B disagree; B alone gives He/H = 0.095.
[9] He^{+}/H^{+} from λ4471 very low and not used.
[10] He^{+}/H^{+} from λ5876 very low and not used.
[11] Considered thin because of low mass.

REFERENCES

[A] Aller *et al.* (1972), NGC 40; Aller *et al.* (1973), NGC 6445; Oliver and Aller (1969), NGC 6302.
[B] Barker (1978*b*).
[D] Danziger, Frogel and Persson (1973).
[K] Paper I and this paper.
[L] Lutz (1977).
[P] Peimbert and Torres-Peimbert (1971).
[T] Torres-Peimbert and Peimbert (1977).

lower limit, which is indicated. The relationship between He/H and T_* is well defined. The nebulae with $\log T_* < 4.65$ are considered to contain neutral He. An exception may be He 2–108, which may be thin, like Ps 1, for which T_* would be a lower limit. Barker (1978*b*) used the existence of strong [S II] emission as a criterion for significant neutral helium. These criteria are quite compatible. If the T_* criterion is used, it includes all the points circled in Barker's Figure 3, plus IC 2149, with the exception of M 2–50, for which the [S II] strength is only an upper limit. If these points are removed, there seems to be little significant trend of He/H with [S II] strength. The right-hand side of Figure 4 shows normalized histograms of He/H for both optically thin (*solid line*) and thick (*dashed line*) nebulae, excluding nebulae with $\log T_* < 4.65$ (but including Ps 1). The ratio of the number of thin to thick nebulae is 2.4. There is no significant difference between the two histograms. Neutral helium seems to present no difficulty as long as we choose nebulae for which $\log T_* \geq 4.65$ ($T_* \sim 44{,}600$ K). One exception may be NGC 3587; see § III*b*. Nebulae with cooler stars are excluded from further discussion, except for Ps 1.

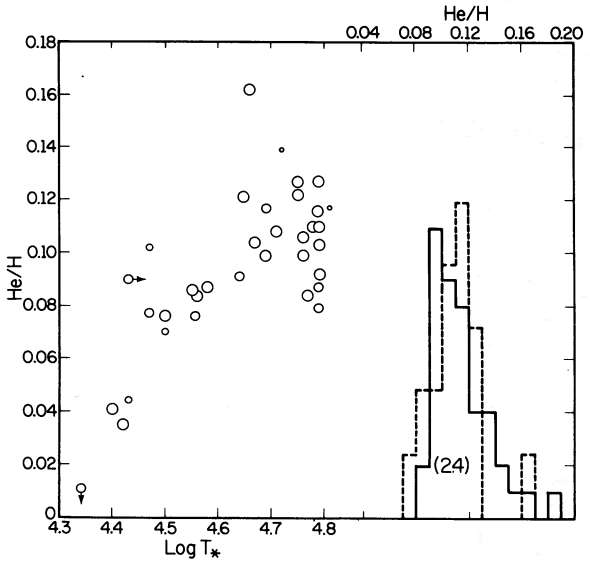

FIG. 4.—Evaluation of neutral helium. *Left*, He/H from combined data (Table 3) plotted against log central star temperature, T_*. See Fig. 3 for interpretation of symbol sizes. *Right*, histograms of the distribution of He/H for optically thin (*solid line*) and optically thick (*dashed line*) nebulae. The normalization factor for thick to thin is given in parentheses.

c) *Correlations with R, |Z|, and $|v_r|$*

Columns (11), (12), and (13) of Table 3 give the distance of the planetary from the galactic center as projected onto the galactic plane, R, distance from the galactic plane, $|Z|$, and radial velocity, $|v_r|$. The values of R and $|Z|$ are found from the distance methods discussed in § III*b*. Values of $|v_r|$ are taken from Perek and Kohoutek (1967) and Boeshaar and Bond (1977). The He/H ratios in column (7) are plotted against R, $|Z|$, and $|v_r|$ in Figures 5, 6, and 7 respectively. The extreme halo nebulae Ps 1, BB 1, and Ha 4–1 are not plotted in Figure 5. The size of the points inversely indicates the error in He/H, according to the legend of Figure 3. In the figures the crosses inside the symbols denote the optically thick nebulae. The circles and boxes in Figure 5 denote Populations I and II, which will be discussed later; they are not separately indicated in Figures 6 and 7.

As expected, the previously described relation between He/H and R is present in Figure 5, since it is present in the individual studies that make it up. Inspection of Figures 6 and 7 shows that the He/H in planetaries behaves similarly with respect to both $|Z|$ and $|v_r|$. The three figures show some common features. Above a certain limit in the X-axis the upper range of He/H shows a rather sudden drop. These limits are 12 kpc for R, 1 kpc for $|Z|$, and about 70 km s^{-1} for $|v_r|$. Below the limits, the range in He/H is greater than

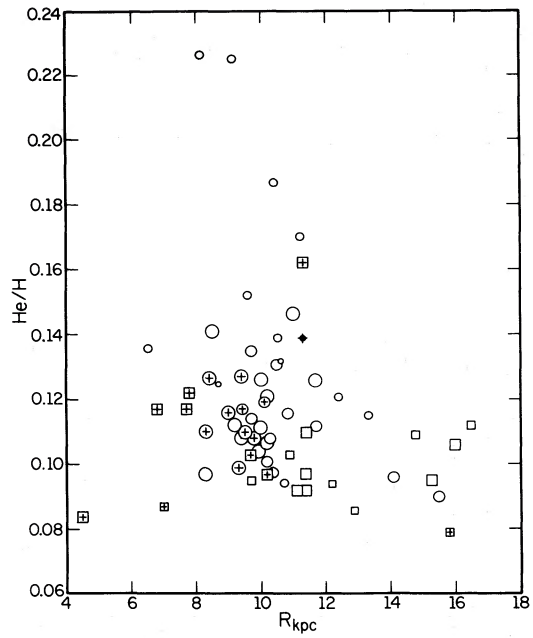

FIG. 5.—The combined He/H results of Table 3 plotted against distance from the galactic center as projected onto the galactic plane, R. See Fig. 3 for an explanation of symbols. *Boxes*, Population II nebulae; *circles*, Population I. The definition of population types for nebulae with $R > 12$ kpc is based upon only $|Z|$ and $|v_r|$ (see text). The extreme halo nebulae Ha 4–1, Ps 1, and BB 1 are not plotted.

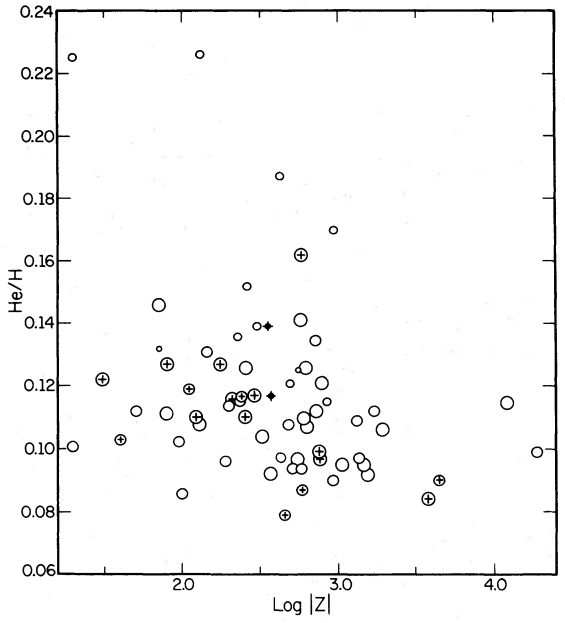

FIG. 6.—The combined He/H results of Table 3 plotted against the log of the distance from the galactic plane, $|Z|$. See Fig. 3 for explanation of symbols.

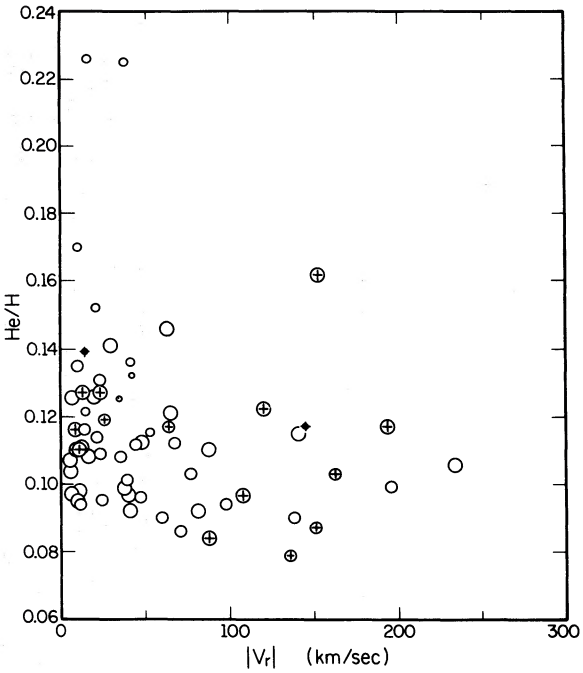

FIG. 7.—The combined He/H results of Table 3 plotted against heliocentric radial velocity, $|v_r|$. See Fig. 3 for explanation of symbols.

it is above the limits. The effect is strongest for $|Z|$ and weakest for $|v_r|$. In addition, there appear to be less conspicuous downward trends to the lower envelopes. The effect is most noticeable for $|v_r|$ and least for R. In the case of R (Fig. 5), the extreme low points scatter rather evenly across the bottom.

Normalized histograms of the distribution of He/H for different sets of planetaries are presented in Figure 8. Nebulae were sorted into bins with He/H ≤ 0.08, $0.08 <$ He/H ≤ 0.09, etc. For the first three, R, $|Z|$, and $|v_r|$ are used for criteria where the solid lines represent planetaries with $R < 12$ kpc, $|Z| < 1.0$ kpc, and $|v_r| <$ km s^{-1}. The dashed lines represent the distributions for objects above these limits. The areas under the dashed lines are normalized to the areas under the solid lines by the factors given in parentheses. The three nebulae with errors greater than or equal to ± 0.02 are excluded from the histograms, as are NGC 6445 and 6302, which were preselected on the basis of their high He/H. The distributions for nebulae above the limits tend to shift to lower He/H, and those for nebulae below the limits tend to have a high helium tail—restatements of points noted above.

Note that if the Cudworth (1974) distance scale were used, the division points on R and $|Z|$ would be larger. For R, the division would be at about 12.5 kpc, except that the high He/H object Hu 1–2 moves to 14.1. A value of just over 14 kpc would represent the outer limit of the division point. For $|Z|$, the division point would be 1.5 kpc.

The fourth histogram (labeled "Morph") shows the distribution of He/H for Greig's (1971) morphological

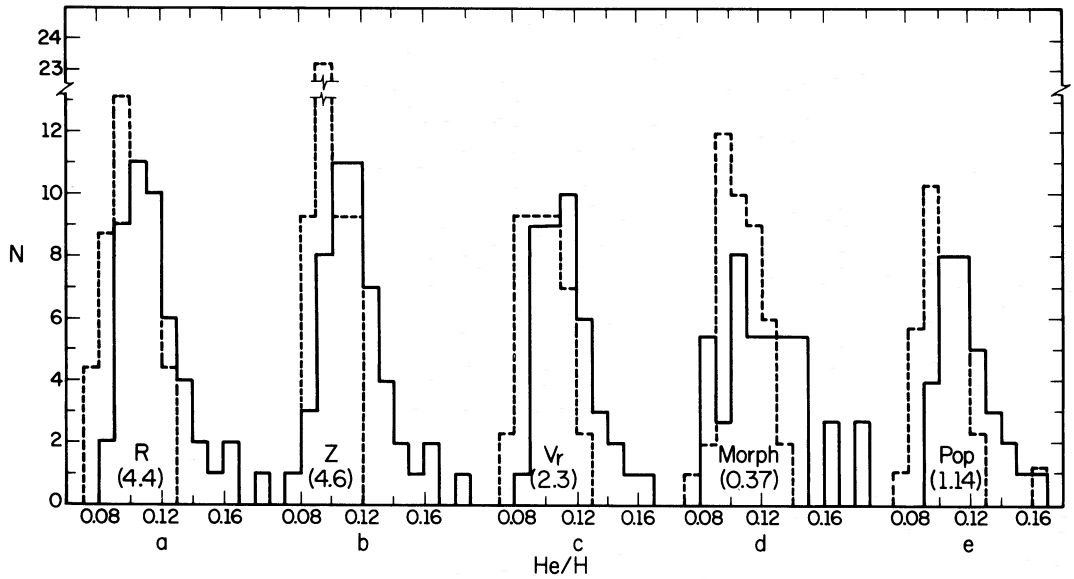

FIG. 8.—Histograms of the distribution of He/H for sets of nebulae, using various parameters as discriminators. In all cases the solid line represents the inner disk, or "Population I" set, the dashed line, the "Population II." The numbers in parentheses give the normalization factors of the Population II set to the Population I set. The nebulae are divided into two sets for each histogram as follows: (*a*) distance from the galactic center, R, at 12 kpc (*solid line* < 12 kpc); (*b*) distance from the galactic plane, $|Z|$, at 1.0 kpc (*solid line* < 1.0 kpc); (*c*) heliocentric radial velocity, $|v_r|$, at 70 km s^{-1} (*solid line* < 70 km s^{-1}); (*d*) Greig's morphological types B (*solid*) and non B (*dashed*); (*e*) population type. If a nebula satisfies any one of the following, $R > 12$ kpc, $|Z| > 1.0$ kpc, $|v_r| > 70$ km s^{-1}, it is called Population II (*dashed line*). The three extreme halo objects are not included in Figure 8*a*. The nebulae NGC 6445 and NGC 6302 and the three lowest weight points are excluded from all figures.

class B and non-B nebulae. The classifications are given in column (14) of Table 3, where "N" refers to non-B objects. In cases where Greig did not classify a nebula, his spectroscopic criteria were used. Greig (1972) shows that B nebulae have Population I characteristics, while non B belong to Population II. In Figure 8, the B nebula distribution is normalized to the non B by one over the number in parentheses. The difference between the two is small, but the effect shown in the three previous histograms does seem to be present, in that the non B nebulae of Population II tend to lack objects with high He/H.

Finally, the nebulae of Table 3 (where $\log T_* \geq 4.65$) were assigned to either Population I or Population II. In order to be called Population II, a nebulae must satisfy *only one* of the three criteria, $R > 12$ kpc, $|Z| > 1.0$ kpc, $|v_r| > 70$ km s^{-1}. This procedure nearly equalizes the number of nebulae within each group. The histograms of the distributions of He/H among the two populations are presented on the right of Figure 8, where the solid line represents Population I and the dashed line Population II. The normalization factor of Population II to Population I is given in parentheses. The effect is now prominent; the Population I set is shifted to higher He/H. If the three nebulae with high errors are included in the histograms, the separation of Population I and Population II becomes more prominent. Note also that both NGC 6445 and 6302 are Population I. In addition, the Population I sample may contain some Population II objects which mimic Population I characteristics; elimination of these would also probably increase the separation. The one prominent exception to the above relation is Me 2–2, which has a very high He/H and a high radial velocity. Other possibly significant exceptions are Cn 2–1 and M 2–27 observed by Webster (1976), both of which have high radial velocities (270 and 180 km s^{-1}) and high He/H (0.14 ± 0.03 and $0.14 \leq 0.02$, respectively). All three of these nebulae are fairly close to the plane, however. Addition of these objects makes the $|v_r|$ relation even weaker. More work should be done on high-velocity nebulae, especially those close to the galactic center.

Averages of He/H for various sets of nebulae are given in Table 4. Column (1) gives the variable, and column (2) gives the criteria as discussed above. Columns (3) and (4) give averages for Populations I and II where these denote the sets of nebulae below and above the limits of column (2), respectively. Column (5) gives the ratio of the Population I average

TABLE 4

AVERAGES OF He/H

VARIABLE (1)	POP. II CRITERION (2)	AVERAGE He/H I (3)	AVERAGE He/H II (4)	RATIO I/II (5)
R.....	>12 kpc	0.117	0.100	1.17
$\|Z\|$.....	> 1 kpc	0.115	0.099	1.16
$\|v_r\|$.....	>70 km s^{-1}	0.114	0.103	1.11
Pop.....	Any of above	0.118	0.103	1.15

to that of the Population II average. Note the similarity of the ratios.

Systematic errors and selection effects are almost impossible to evaluate. A plot of He/H against distance shows no correlation. If anything, selection should work the other way. Discovery and observation should be more complete toward the anticenter where there is less interstellar dust. Consequently, high He/H objects there should not be hidden.

One systematic effect involves the calculation of Z and R. The distances of the optically thin nebulae are based upon an assumption of constant planetary mass. But if the He/H ratios reflect systematic stellar mass variations, as suggested in the next section, then the masses of the planetaries might vary also. If the masses of Population II planetaries are smaller, we would systematically overestimate R and Z and the limits upon which the population types are based.

d) Helium Enrichment and Galactic Gradients

The purpose of this section is to suggest explanations for the correlations seen in Figures 5 through 8. T assumed that the apparent gradient involving He/H and R was due to an interstellar galactic gradient in He/H. However, there are two points which must be considered. First, the variation in He/H, especially for nebulae with $R < 12$ kpc, is much larger than the error in He/H, which is typically less than ± 0.01. The large range for a given value of R implies that nebulae with He/H above the minimum are enriched in helium. This comment applies to the correlations of He/H with $|Z|$ and $|v_r|$ as well. Second, from theoretical considerations, many planetaries *should* be enriched with helium. For stars with initial masses between 3 and 8 $M_\odot$, it is known that the amount of fresh helium brought to the surface at the beginning of the asymptotic branch phase increases with increasing initial (main sequence) stellar mass (Iben 1977). Stars initially less massive than about 3 $M_\odot$ do not experience this helium enhancement phase that accompanies the formation of an electron-degenerate carbon-oxygen core, and stars initially more massive than about 8 $M_\odot$ ignite carbon at their centers before the helium enhancement can occur. Thus one would not expect planetaries whose progenitors are less massive than about 3 $M_\odot$ to exhibit a He/H ratio much different from their initial main-sequence values, and would expect those planetaries with the largest He/H ratios to have as main-sequence progenitor stars with masses near the upper end of the 3–8 $M_\odot$ range.

The distribution of He/H in Figures 5, 6, and 7 may then reflect two effects at work. The first is the possibility that there is a true interstellar gradient, as suggested by T and others, which controls the helium content out of which the parent star was formed. Second, given that planetaries commonly are enriched in helium, the apparent gradients and the difference in He/H ranges above and below the limits ($R = 12$ kpc, $|Z| = 1$ kpc, $|v_r| = 70$ km s^{-1}) may reflect gradients in the types of stars that produce the planetaries.

It is clear from earlier work (e.g., Smith 1975) that the abundances of heavy elements decrease as we proceed outward in a spiral galaxy. T and Hawley (1978) show the effect reflected in O/H ratios of planetaries and diffuse nebulae, respectively, and Mayer (1976) shows it in the galactic metal gradient. Shields and Tinsley (1976) also show that the maximum effective temperatures of stars increase radially outward. Clearly, the opacities of stars are dependent upon distance from the galactic center. The nebulae in the outer parts of the Galaxy (beyond 12 kpc from the galactic center, and especially beyond 14 kpc) tend to have Population II or halo characteristics. That is, they also have high $|Z|$ or $|v_r|$. The masses of halo stars are generally lower than the masses of disk stars. Iben (1974), for example, points out from analysis of variables that halo stars tend to have similar low masses, but that disk stars have a wide range of masses which extend to higher values. It is reasonable to suppose that the He/H ratios of planetaries are dependent on both the masses and opacities of the parent stars. These should determine (1) how much helium is mixed upward prior to injection, and (2) the point of lift-off of the planetary shell. If we have a wide range of stellar masses for $R < 12$ kpc and $|Z| < 1$ kpc, we would expect a large range in He/H. But if stars for $R > 12$ kpc, $|Z| > 1$ kpc have generally lower masses, the He/H values will also be lower, and the range smaller.

We now examine both of the above hypotheses; they may in fact be difficult to separate from one another. If the data presented in Figure 5 are interpreted strictly as an interstellar gradient, with the large scatter being due to observational error, then an unweighted least-squares fit (excluding NGC 6302, NGC 6445, and the points with errors ≥ 0.02) gives a gradient of -0.0014/kpc. (The optically thin points alone give -0.0031/kpc). However, the arguments presented above indicate that most of the planetaries above the minimum for a given R (or $|Z|$, $|v_r|$) are enriched in helium. We might expect, then, that the minimum He/H observed at a given value of R would be the original interstellar value at R. That is, the objects with minimum He/H show no enrichment. If there were an interstellar He/H gradient, we would expect the minimum He/H to increase with decreasing R. Examination of Figure 5 shows, however, that the points scatter rather evenly across the bottom of the graph. If the two low He/H points between 4 and 8 kpc are thrown out, it is still unlikely that the slope of the lower envelope could be any larger than the average gradient of -0.0014/kpc derived above, which is nearly 4 times less than that suggested by T.

e) Disk-Halo Differences and the Radial Gradient

It is evident from Figure 8*e* that the minimum He/H for Population II is somewhat less than the minimum for Population I. The difference between the two populations is clearer if He/H is plotted against nebular excitation, as in Figure 9. Here the independent variable is log T_* for nebulae with weak or no He II lines, and Ex = He^{2+}/He for higher-excitation objects. The two

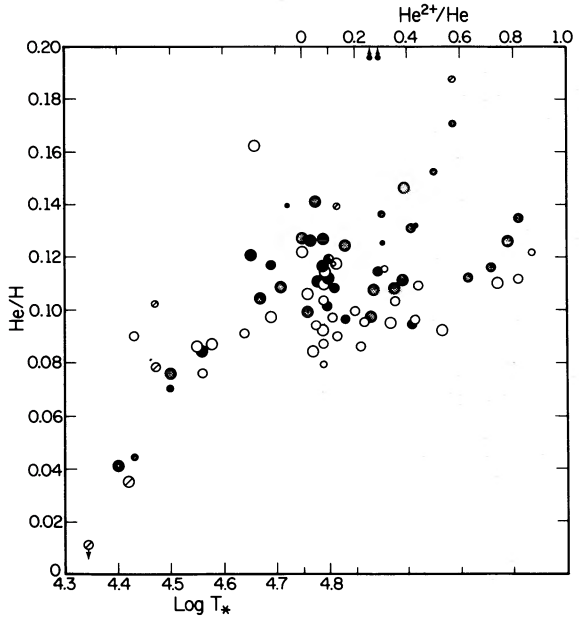

FIG. 9.—He/H plotted against log T_* and Ex = He^{2+}/He. Population I nebulae are plotted as closed circles, Population II (defined in legend, Fig. 8) as open circles. Nebulae for which the population is not known are indicated by a diagonal slash.

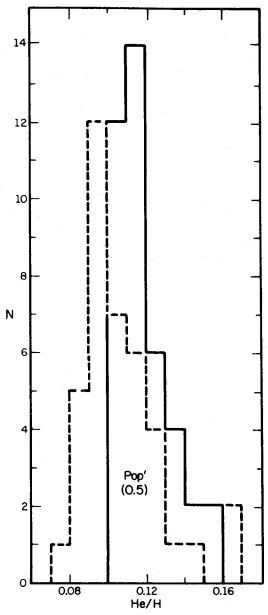

FIG. 10.—Histograms for the distribution of He/H for redefined population types I′ and II′, where Population I′ has $R < 12$ kpc, $|v_r| < 70$ km s^{-1}, $|Z| < 400$ pc. The number in parentheses is the ratio of the number of Population I′ to II′. The histograms are normalized to Population II′.

scales are joined at log $T_* = 4.75$ (see Kaler 1978*a* for a full explanation of this scheme). In Figure 9, the Population I nebulae are plotted as filled circles, the Population II as open. We see here that the minimum for the Population I points lies above the minimum for the Population II points. This feature holds even if the four nebulae above $R = 12$ kpc with $|Z| <$ 1 kpc, $|v_r| < 70$ km s^{-1} are considered Population I. If we assume that the nebulae of each population with minimum He/H are individually not enriched, then the average helium in the general disk as defined by $|Z| <$ 1000 pc is enriched over that of the halo by about 10%–15%, which is similar to the ratios of averages presented in Table 4.

The difference between the disk and the halo is even more marked if Population I is defined more restrictively, such that $|Z| < 400$ pc. Figure 10 shows a histogram of the distributions of He/H for nebulae belonging to each class, where now we define a Population I′ which consists of nebulae with $R < 12$ kpc, $|Z| < 400$ pc, $|v_r| < 70$ km s^{-1}. The clear difference in the Population I′ and II′ distributions is reflected in the systematic variation of the minimum He/H in Figure 6, where He/H is plotted against log $|Z|$. There are far fewer nebulae with He/H < 0.10 for log $|Z| <$ 2.6 ($|Z| < 400$ pc) than there are above log $|Z| =$ 2.6. And the three nebulae that have He/H < 0.10 and log $|Z| < 2.6$ are all Population II as defined by $|v_r|$ and R. Of the Population II′ nebulae (redefined with $|Z| > 400$ pc), half have He/H < 0.10, whereas all of the Population I′ nebulae have He/H > 0.10.

The difference between the two sets of histograms shown in Figure 8*e* and Figure 10 is consistent with a continuous gradient of He/H in $|Z|$. As we restrict the population-dividing $|Z|$ limit more closely to the galactic plane, the difference in the minimum He/H between Populations I and II increases. Both population sets II and II′ include the extreme minimum values which start at about 0.08. Population I′ has no values of He/H < 0.10 because it is tightly restricted to the disk, whereas Population I has four points between 0.083 and 0.10 because it extends farther into the halo. If we examine the minima for Populations I′ and II′ and allow for the typical errors of $\sim \pm 0.006$ for these nebulae, we find that the original He/H of the extreme halo is ~ 0.085, and the current interstellar He/H of the disk is ~ 0.105. The He/H of the extreme halo is similar to that of the Magellanic Clouds as found by Peimbert and Torres-Peimbert (1974, 1976), which is 0.084 ± 0.005 and 0.078 ± 0.005 for the Large and Small Clouds, respectively. The minimum He/H for the disk with $|Z| < 400$ pc is similar to that of the Orion Nebula derived by Peimbert, Torres-Peimbert, and Rayo (1978) and Hawley (1978) to be 0.105 and 0.112, respectively. The extreme range in He/H for a $|Z|$ gradient amounts to perhaps something over a 20% variation.

This hypothesis is not entirely consistent with the three extreme halo nebulae BB 1, Ha 4–1, and Ps 1 (see Table 3). These three nebulae might be expected to have minimum He/H, since they are so far from the plane, but the measured He/H is 0.099, 0.115, and 0.09, respectively. Perhaps BB 1 and Ha 4–1 show effects of helium enrichment.

Two other significant features which appear in Figure 9 should be mentioned here. First, starting at

Ex = 0, there is a general upward trend in the lower envelope of He/H as Ex increases, also pointed out by Kaler (1978*c*). Second, if we follow the curve upward from $\log T_* \approx 4.4$, there is a sudden drop in minimum He/H at $\log T_* \approx 4.75$. That is, there is a deficiency of low He/H at $\log T_* = 4.7$ as compared with $\log T_* = 4.75$. The causes of these features are not known, but there are a variety of possible explanations. The first feature may be due to observational selection. The highest-excitation nebulae have weak He I lines, which may only have been detected for nebulae with high He/H. We need more observations of high-excitation objects. The second feature may be due only to chance effects from a small sample; there are few nebulae at $\log T_* \approx 4.6$ to 4.7. We must also consider the possibility that both features may be due to the presence of neutral helium at $\log T_* \approx 4.8$, which would result in erroneously low values of He/H. The nebulae with low He/H at $\log T_* \approx 4.8$ are Population II, and if these also contained neutral helium, much of the difference in minimum He/H between Population I and Population II would disappear. However, there are good reasons to believe that neutral helium is not a problem. The first is the histogram in Figure 4 discussed earlier. Second, if we isolate the planetaries between with $4.75 \leq \log T_* < 4.83$, they show no systematic trends with regard to whether they are designated *thick* or *thin* in Table 3, column (10). That is, there are as many thick nebulae at high He/H as there are at low. However, the lowest three points are thick. There is also evidence that one of these points, NGC 3587, may in fact contain neutral helium; see § III*b*. Third, if neutral helium is the problem, we must explain why it seems to be confined mostly to Population II objects. Systematic galactic effects may also be involved. For example, if we consider only the set of Population I′ nebulae, the first feature described above practically disappears. Clearly, the features in Figure 9 will have to be examined much more closely with an increased quantity of data. The existence of neutral helium cannot yet be ruled out, and the problem must be studied more extensively.

Return now to Figure 5 and to the original definition of population type, except that here nebulae beyond 12 kpc are called Population I if they satisfy both the criteria $|Z| < 1$ kpc, $|v_r| < 70$ km s^{-1}. Note that seven of the 11 points with $R > 12$ kpc are defined as Population II on the basis of $|Z|$ or $|v_r|$, four on the basis of $|Z|$ alone. If we use the alternate definitions for Populations I′ and II′, 10 of the 11 are Population II′, nine on the basis of $|Z|$ alone. The generally lower He/H for nebulae with $R > 12$ kpc may at least in part reflect the difference in minimum He/H between population types, or between the halo and the disk.

If the He/H of the Population II nebulae are multiplied by 1.15 (the rough difference in minima between Populations I and II, which is about the same as the ratios presented in Table 4), some of the appearance of a gradient in R disappears, and there is no evidence of a gradient in minimum He/H with R. In addition, if we look at minimum He/H of only the Population I points of Figure 5 (*circles*), no gradient is evident. Clearly, a small one could still exist within the scatter; the number of points that define the minimum is too small.

Now, given the difference between the disk and the halo, is there evidence that the Population I nebulae are more enriched in He as a class than those of Population II? Consider again the difference between Figures 8*e* and 10. The spread in He/H for Population II′ is greater than it is for Population II. Since Population II′ extends closer to the plane, it will include objects that start at higher He/H than will Population II, and probably will also include stars of higher mass which can produce more highly enriched planetaries.

If we ignore Me 2–2, the highest He/H among Population II is 0.122. If this highest point is produced by a nebula with minimum He/H ≈ 0.085, then the enrichment factor is about 45%, which is about the same as that seen for Population I′, implying that Population II nebulae are also enriched, and implying that there is a range of stellar masses. However, because we have already established the likelihood of a continuous interstellar $|Z|$ gradient, it seems likely that the high He/H nebulae of Population II originally had a value of He/H higher than the minimum, and are less enriched.

Let us take a conservative approach, and multiply the Population II distribution in Figure 8*e* by 1.15, the approximate maximum ratio of the minima. The Population I and II distributions are then rather similar. Still, the very highest He/H ratios are missing from Population II. If the He/H of Population II are multiplied by 1.15, the highest value (except for Me 2–2) is 0.14. Population I has four nebulae above this value (six, if NGC 6302 and NGC 6445 are included), Population II only one. Note, however, Webster's (1976) two points with high He/H and high $|v_r|$. Clearly, at this point we are hampered by a small sample.

A similar effect is seen in the distributions for $|Z|$ and R. If the Population II points (*boxes*) in Figure 5 are multiplied by 1.15, there is still a lack of high He/H for $R > 12$ kpc. Even with this correction we would expect three to four nebulae with (He/H) × 1.15 > 0.13 for $R > 12$ kpc, but there are none. In this case, Webster's (1976) points fit into the above statement, since they are close to the galactic center. However, if all the points with $R > 12$ kpc are raised by a factor of 1.15, there are two with He/H > 0.13. Still, the very highest values are missing. And if the Population II nebulae of Figure 6, where He/H is plotted against $|Z|$, are increased by a factor of 1.15, we would expect 3 nebulae with (He/H) × 1.15 > 0.135 for $|Z| >$ 1 kpc, but there are none. The distributions in He/H with $|v_r|$ seen in Figure 7 do not show this effect. The range for nebulae with $|v_r| > 70$ km s^{-1} is about the same as that for the slower nebulae, especially if Webster's (1976) points are included.

In summary, both populations, as defined in this paper, show evidence for enrichment. But there is evidence that the Population I nebulae can be more highly enriched than those of Population II, especially when we consider that the highest He/H Population II objects may not be enriched from the minimum He/H observed, but from some higher value. This fact is con-

sistent with the greater range of masses expected for Population I. The evidence for greater Population I enrichment is not clear-cut, however, and more observations are needed. Nevertheless, since most of the nebulae with $R > 12$ kpc are Population II, the effect adds to the appearance of a radial gradient.

V. SUMMARY AND CONCLUSIONS

This paper confirms the apparent radial gradient in He/H found by D'Odorico, Peimbert, and Sabbadin (1976) and by Torres-Peimbert and Peimbert (1977), both from new photoelectric photometry and from a combination of the major sets of data. Similar apparent negative gradients are also seen with respect to distance from the galactic plane and radial velocity. The last is the weakest, since there are some high-velocity nebulae (this paper; Webster 1976) which show high He/H.

The interpretation of the radial gradient, based upon considerably more data, is different from that of the other authors. The observed apparent radial gradient can be explained by a combination of two effects.

1. There is evidence for a population gradient in He/H which is probably continuous as we proceed from the central inner plane of the galaxy to the extreme halo. The current interstellar He/H of the disk may be 20% higher than the original He/H of the halo objects, which is more like that of the Magellanic Clouds. This difference will appear as a radial gradient because of the high proportion of Population II nebulae (as defined by $|Z|$ and $|v_r|$) for $R > 12$ kpc.

2. Values of He/H above the minimum for a given value of R, $|Z|$, or $|v_r|$ are produced by helium enrichment of the nebula by fusion processes within the parent star. The mass range of stars within 12 kpc of the galactic center may be larger than it is for stars with $R > 12$ kpc, and consequently the range in He/H is greater. The relative importance of these two effects is not known.

If an interstellar radial gradient is present it is too small to be detected by the present set of nebulae, and at the most it is less than about one-fourth that suggested by T. There is no detectable variation in the minimum observed He/H for planetaries as a function of distance from the galactic center as projected onto the plane after the effects of a gradient perpendicular to the plane have been accounted for. This finding is in accord with the lack of a gradient found from diffuse nebulae in our Galaxy by Hawley (1978).

By the time the 78 planetary nebulae have been divided into the various subgroups, there are often only small numbers left in a sample. Further observations are clearly needed for (1) nebulae greater than 12 kpc (on the Cahn-Kaler scale) and particularly those less than 8 kpc from the galactic center; an interstellar gradient cannot be ruled out until we can probe closer to the center; (2) planetaries with high radial velocity, especially those near the galactic center; and (3) high-excitation nebulae.

In addition, searches should be made for more nebulae with high He/H.

This work was supported by National Science Foundation grant AST 76-20840 to the University of Illinois. I would like to thank Drs. S. Torres-Peimbert, M. Peimbert, T. Barker, and S. Hawley, who provided data and manuscripts in advance of publication. I would also like to thank Drs. I. Iben and J. Truran for valuable discussion, and Drs. J. Lutz and S. Wyatt for helpful comments on the manuscript.

REFERENCES

Aller, L. H. 1968, in *IAU Symposium No. 34, Planetary Nebulae*, ed. D. E. Osterbrock and C. R. O'Dell (Dordrecht: Reidel), p. 339.
———. 1976, *Pub. A.S.P.*, **88**, 574.
Aller, L. H., Czyzak, S. J., Buerger, E. G., and Lee, P. 1972, *Ap. J.*, **172**, 361.
Aller, L. H., Czyzak, S. J., Craine, E., and Kaler, J. B. 1973, *Ap. J.*, **182**, 509.
Barker, T. 1978*a*, *Ap. J.*, **219**, 914 (B).
———. 1978*b*, *Ap. J.*, **220**, 193.
Boeshaar, G. O., and Bond, H. E. 1977, *Ap. J.*, **213**, 421.
Brocklehurst, M. 1971, *M.N.R.A.S.*, **153**, 471.
———. 1972, *M.N.R.A.S.*, **157**, 211.
Cahn, J. H., and Kaler, J. B. 1971, *Ap. J. Suppl.*, **22**, 319.
Capriotti, E. R., and Daub, C. T. 1960, *Ap. J.*, **132**, 677.
Collins, G. W., Daub, C. T., and O'Dell, C. R. 1961, *Ap. J.*, **133**, 471.
Cox, D. P., and Daltabuit, E. 1971, *Ap. J.*, **167**, 257.
Cudworth, K. M. 1974, *A.J.*, **79**, 1384.
Danziger, I. J., Frogel, J. A., and Persson, S. E. 1973, *Ap. J. (Letters)*, **184**, L29.
D'Odorico, S., Peimbert, M., and Sabbadin, F. 1976, *Astr. Ap.*, **47**, 341.
Greig, W. E. 1971, *Astr. Ap.*, **10**, 161.
———. 1972, *Astr. Ap.*, **18**, 70.
Hawley, S. A. 1978, *Ap. J.*, **224**, 417.
Hawley, S. A., and Miller, J. S. 1978, *Ap. J.*, **220**, 609.
Hummer, D. G., and Seaton, M. J. 1964, *M.N.R.A.S.*, **127**, 217.
Iben, I., Jr. 1974, in *IAU Symposium No. 59, Stellar Instability and Evolution*, ed. P. Ledoux, A. Noels, and A. W. Rodgers (Dordrecht: Reidel), p. 3.
———. 1977, in *Advanced Stages in Stellar Evolution*, ed. P. Bouvier and A. Maeder (Geneva: Geneva Observatory), p. 1.
Kaler, J. B. 1974, *Ap. J. (Letters)*, **188**, L15.
———. 1976*a*, *Ap. J.*, **210**, 113 (Paper I).
———. 1976*b*, *Ap. J. Suppl.*, **31**, 517 (KC).
———. 1976*c*, *Ap. J.*, **210**, 843.
———. 1978*a*, *Ap. J.*, **225**, 527.
———. 1978*b*, *Ap. J.*, **220**, 887.
———. 1978*c*, in *IAU Symposium No. 76, Planetary Nebulae*, ed. Y. Terzian (Dordrecht: Reidel), p. 235.
Lutz, J. H. 1977, *Pub. A.S.P.*, **89**, 10.
Mayer, M. 1976, *Astr. Ap.*, **48**, 301.
Miller, J. S., and Mathews, W. G. 1972, *Ap. J.*, **172**, 593.
O'Dell, C. R. 1962, *Ap. J.*, **135**, 371.
———. 1963, *Ap. J.*, **161**, 1015.
Oke, J. B., and Schild, R. E. 1970, *Ap. J.*, **161**, 1015.
Oliver, J. P., and Aller, L. H. 1969, *Ap. J.*, **157**, 601.
Peimbert, M. 1973, *Mém. Soc. Roy, Sci. Liège*, 6th Ser., **5**, 79.
Peimbert, M., and Torres-Peimbert, S. 1971, *Ap. J.*, **168**, 413 (P).
———. 1974, *Ap. J.*, **193**, 327.
———. 1976, *Ap. J.*, **203**, 581.
Peimbert, M., Torres-Peimbert, S., and Rayo, J. F. 1978, *Ap. J.*, **220**, 516.

Perek, L., and Kohoutek, L. 1967, *Catalog of Galactic Planetary Nebulae* (Prague: Czechoslovakian Academy of Sciences).
Robbins, R. R. 1968, *Ap. J.*, **151**, 511.
Shields, G. A., and Searle, L. 1978, *Ap. J.*, **222**, 821.
Shields, G. A., and Tinsley, B. M. 1976, *Ap. J.*, **203**, 66.
Smith, H. E. 1975, *Ap. J.*, **199**, 591.
Torres-Peimbert, S., and Peimbert, M. 1977, *Rev. Mexicana Astr. Ap.*, **2**, 181 (T).
Vorontsov-Vel'yaminov, B. A., Kostjakova, E. B., Dokuchaeva, O. D., and Archipova, U. P. 1965, *Astr. Zh.*, **42**, 730.
Webster, B. L. 1976, *M.N.R.A.S.*, **174**, 513.

JAMES B. KALER: University of Illinois Observatory, Urbana, IL 61801